Special Issue Paper

Development of Cobalt Sulfide-graphene Composite for Supercapacitor Applications

Milan Jana*, Pranab Samanta*, Naresh Chandra Murmu*, Nam Hoon Kim**,
Tapas Kuila*[†], Joong Hee Lee**[†]

ABSTRACT: Co_9S_8/reduced graphene (CSRG) has been prepared by a facile two step hydrothermal method and used as a supercapacitor electrode material. It is anticipated that the Co_9S_8 and reduced graphene oxide (RGO) would serve as a spacer material to each other to stop the agglomeration and simultaneous contribution of electrical double layer capacitance (RGO) and pseudocapacitance (Co_9S_8) would provide high electrochemical properties. The chemical analysis has been done by Fourier transform infrared spectroscopy and the morphology is characterised by field emission scanning electron microscopy. CSRG shows a high electrical conductivity of 98 S m^{-1}. The symmetric supercapacitor shows a specific capacitance of ~728 F g^{-1} with a current density of 2 A g^{-1}. CSRG also showed an energy density of 25.2 Wh kg^{-1} with a power density of 1000 W kg^{-1}.

Key Words: Co_9S_8/reduced graphene oxide, Supercapacitor, Energy density, Power density

1. INTRODUCTION

The increasing demand of energy in the 21st century has been triggered off numerous research efforts in energy conversion and storage from the renewable and green resources. Solar power and wind energy can be the substitute of the fossil fuel by storing these energies efficiently for future applications [1-7]. Electrochemical capacitors (EDLC) can complement or even substitute batteries in energy storage applications [7]. Colossal research attempts have been paid on supercapacitor electrode materials and electrolyte through the last two decades to get its application in reality [1-9]. Different electro active materials such as Nio, Co_3O_4, MnO_2, Cuo, CoS, etc. have been examined as supercapacitors electrode [8,9]. However the energy density and power density obtained from these electrode materials were very low due to their lower operating voltage. The newly found carbonaceous material graphene attracted the research scientists due to its higher surface area, good electrical conductivity and lower production cost and

can survive as a very good electrochemical material for supercapacitors electrode [9]. It is hoped that the interrogation of metal oxides or metal sulfides with graphene can enhance the supercapacitor properties [10,11]. Metal sulfide has been studied very less as supercapacitor electrode materials. Lou *et al.* Reported a CoS_2 supercapacitor electrode with a specific capacitance ~1040 F g^{-1} at current density of 0.5 A g^{-1} [12]. Pu *et al.* prepared a Co_9S_8-based supercapacitor with a specific capacitance of ~1775 F g^{-1} at 4 A g^{-1} [8]. Herein, we developed Co_9S_8/reduced graphene composite (CSRG) by a two step hydrothermal reaction and used as supercapacitor electrode material. The CSRG electrodes exhibit a very high specific capacitance of ~728 F g^{-1} at a current density of 2 A g^{-1}.

2. EXPERIMENTAL

2.1 Materials

Natural flake graphite and polyvinylidene fluoride (PVDF) was obtained from Sigma-Aldrich. Hydrochloric acid, potas-

sium permanganate, hydrogen peroxide, potassium hydroxide, sulphuric acid and N,N-dimethyle formamide were purchased from Merck, Mumbai, India. Cobalt chloride, urea and sodium sulfide were obtained from SRL, Mumbai, India. Nickel foam and carbon black was obtained from Shanghai Winfay New Material Co., Ltd, China and MTI Corporation, USA, respectively.

2.2 Synthesis of Co_9S_8 nano rods on reduced graphene surface

Graphene oxide (GO) is prepared by a modified Hummers method. Around 190 mg $CoCl_2 \cdot 6H_2O$ was added to 60 ml of graphene oxide solution (1 mg ml^{-1})) and sonicated 30 minutes. 240 mg urea was added to the solution and it was transferred to a 100 ml stainless steel autoclave. The autoclave was then heated for 8 h at 95℃ in hot air oven. The collected product was treated hydrothermally for 2 h with 0.2 M Na_2S solution. It is anticipated that the Co^{2+} ions are adsorbed on the GO surface due to the electrostatic attraction force of oxidative debris.

Urea plays an important role to provide hydroxyl groups to form the intermediate $Co(CO)_{0.35}Cl_{0.20}(OH)_{1.10}$. The GO is reduced by the ammonia released during the hydrolysis of urea. The adsorbed Co^{2+} ions has been converted to an intermediate $Co(CO)_{0.35}Cl_{0.20}(OH)_{1.10}$ and GO is reduced to RGO during the first step of the reaction in presence of urea at 95 C. The S^{2-} ions reacts to the intermediate The $Co(CO)_{0.35}Cl_{0.20}(OH)_{1.10}$ to form Co_9S_8 during the second step of reaction in presence of Na_2S at 120 C. The schematic for the probable formation mechanism of CSRG is presented in Fig. 1.

2.3 Characterization

Fourier transform infrared spectroscopy (FT-IR) of the sample was characterised by Nicolet 6700 spectrometer (Thermo scientific, USA). The morphology was characterised by field emission scanning microscopy (FE-SEM) using Σigma HD, Carl Zeiss, Germany. Transmission electron microscopy (TEM) and selected area electron diffraction (SAED) of CSRG was obtained from JEM-2100 FS (JEOL, Japan). The electrical
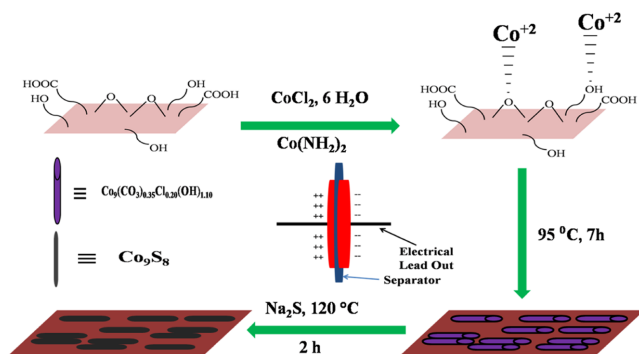
conductivity of the samples was measured by a KEITHLEY Delta arrangement consisting of AC & DC current source, model: 6221 and Nanovoltmeter, model: 2182A. The cyclic voltammetry (CV), galvanostatic charge-discharge and electrochemical impedance spectroscopy (EIS) were performed in a PARSTAT 4000 (Princeton Applied Research, USA) electrochemical workstation in a two electrode system. The electrode was prepared through drop casting electrode materials on 1 cm diameter nickel foam substrate. CSRG, carbon black and polyvinylidene fluoride were mixed properly with a mass ratio of 8 : 1.5 : 0.5 in dimethylformamide. The slurry was drop casted over the Nickel foam (current collector). Whatman 42 filter paper was used as the separator to design a symmetric supercapacitor, where 6 (M) KOH was used as electrolyte.

3. RESULTS AND DISCUSSION

3.1 FT-IR Spectra analysis

Fig. 2 shows the FT-IR spectrum of GO and CSRG composite. The stretching vibration peak of -OH functional group of water appeared at 3430 cm^{-1}. The stretching vibration peaks of alkoxy and epoxy groups of GO appeared at 1060 and 1240 cm^{-1}. The peak corresponding to carboxylic groups appeared at 1720 cm^{-1} of GO [13]. The peak at 1140 cm^{-1} in the spectra of CSRG indicated the bending vibration peak of sulfonated group of cobalt sulfide [11]. The stretching vibration of Co atom in Co_9S_8 was represented by the peak at 620 cm^{-1} [11]. Both the characteristic peaks of Co_9S_8 nanorods were present in the spectrum of CSRG, suggested the successful decoration of Co_9S_8 nanorods on the reduced graphene (RGO) surfaces. The peaks corresponding to oxygen functional groups of GO were either decreased or removed from the FT-IR spectrum of CSRG. It suggested the reduction of GO during the hydrothermal process.
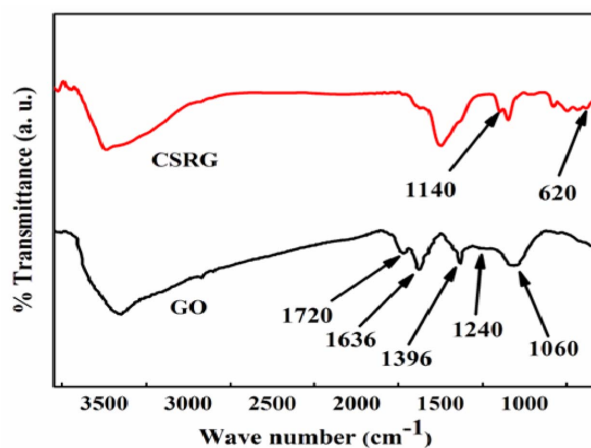

Fig. 1. Schematic representation of formation mechanism of Co_9S_8 nano particles on RGO

Fig. 2. FT-IR spectra of CSRG and GO
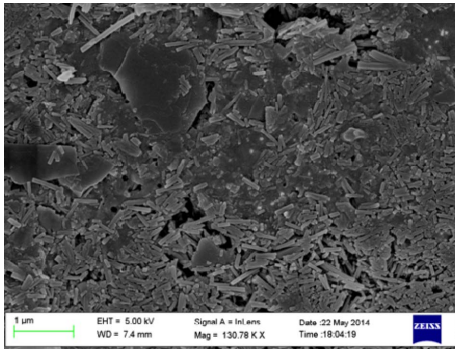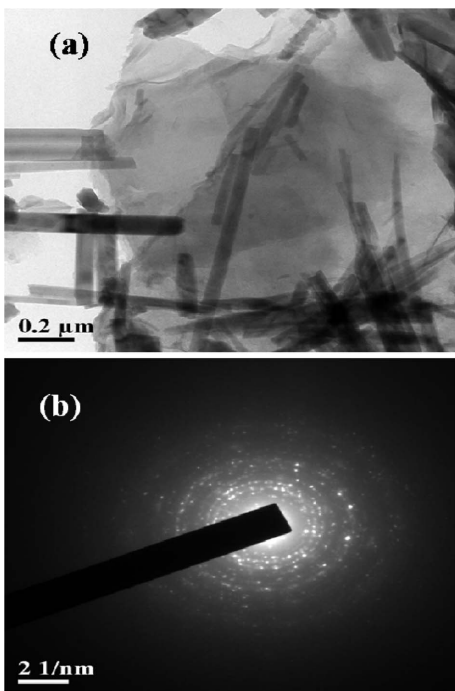
Fig. 3. FE-SEM image of CSRG

Fig. 4. (a) TEM and (b) SAED pattern image of CSRG

3.2 FE-SEM and TEM analysis

Fig. 3 represents the FE-SEM image of CSRG. It clearly revealed the decorating of Co_9S_8 nanorods on RGO surfaces. The typical porous nature of CSRG helped to improve the electrochemical performances. The TEM image of CSRG is presented in the Fig. 4(a). The TEM image reveals that the Co_9S_8 nanorods are randomly decorated over RGO sheets. The well separated Co_9S_8 nanorods can get a good access of electrolyte to contribute pseudocapacitance to the EDLC of RGO. The polycrystalline nature of the CSRG (as experienced from the SAED pattern image) further confirms the hybridization of Co_9S_8 and RGO.

3.3 Electrical conductivity measurements

The electrical conductivity was measured by a four probe method using the formula

$$\text{Electrical conductivity} = 1/(4.53 \times R \times d) \tag{1}$$

Where R is the resistance and d is the thickness. The conductivity of GO, pure Co_9S_8 and CSRG were found to be $\sim9.5 \times 10^{-2}$, 1.4 and 98 S m^{-1} respectively. The increment in electrical conductivity in CSRG than pure Co_9S_8 and GO confirmed the reduction of GO and successful anchoring of Co_9S_8 nano rods on to the conjugated sp^2 network of RGO.

3.4 Electrochemical performances

The electrochemical performance of CSRG and pure is experienced by designing two electrode based supercapacitor devices, where 6 (M) KOH has been used electrolyte. The CV response of pure Co_9S_8 and CSRG at scan rate of 50 mV s^{-1} at the voltage range of 0-1 V are shown in Fig. 5(a). Theoretically an ideal supercapacitor should show a rectangular nearly CV curve with reversible cathodic and anodic loops [7,15]. The curve of pure Co_9S_8 was deformed from its reversible nature at higher voltage range ~0.8 V. Whereas, the CV loop of CSRG was comparably reversible and mirror image like in nature. The CV loops of the CSRG showed higher current response than pure Co_9S_8. It clearly revealed that CSRG afford greater electrochemical performances than pure Co_9S_8 [15,16]. The quasi-rectangular CV curves of CSRG confirm the reversible nature of the redox reactions. The galvanostatic charge-dis-
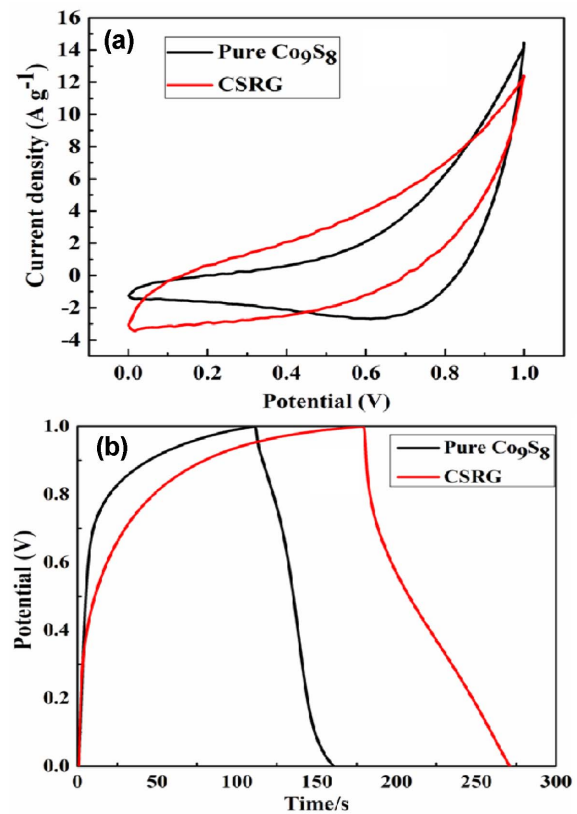

Fig. 5. (a) Cyclic voltammetry curves, (b) galvanostatic charge-discharge curves of CSRG and pure Co_9S_8
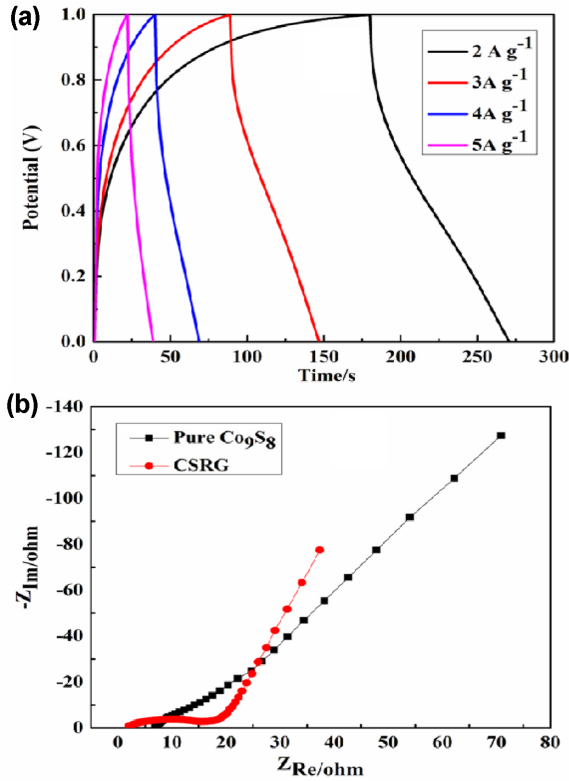
(a)

(b)

Fig. 6. (a) Galvanostatic charge-discharge curves of CSRG at different current densities, (b) Nyquist plot of CSRG and pure Co_9S_8

charge curves of pure Co_9S_8 and CSRG are represented in Fig. 5(b) at current density of 2 A g^{-1}.

The coulombic efficiency (CE) was calculated by using the equation

$$CE = (discharging\ time/charging\ time) \times 100 \qquad (2)$$

The CE was found to be 41 and 50% respectively for pure Co_9S_8 and CSRG. The increment in CE may be due to the introduction of electrical double layer nature (EDL) of RGO to the redox nature of Co_9S_8. The specific capacitance (SC) of the pure Co_9S_8 and CSRG was calculated from the charge-discharge curves using the formula

$$SC = 4 \times I_m \times (\Delta t/\Delta V) \qquad (3)$$

Where, I_m is the current density, Δt is the discharging time, ΔV is the operating voltage. The SC of pure Co_9S_8 was found to be 392 F g^{-1}, whereas the SC of CSRG was calculated to be 728 F g^{-1} at a current density of 2 A g^{-1}.

Fig. 6(a) shows the charge-discharge curves of CSRG at different current densities. Interestingly, it is notified that the CE values increased with increasing the current densities and found to be ~78% at high current density of 5 A g^{-1}. The SC values of CSRG have been found to be ~684, 480, and 340 F g^{-1} at current densities of ~3, 4 and 5 A g^{-1}. The charge storage mechanism of Co_9S_8 in the KOH medium can be explained by
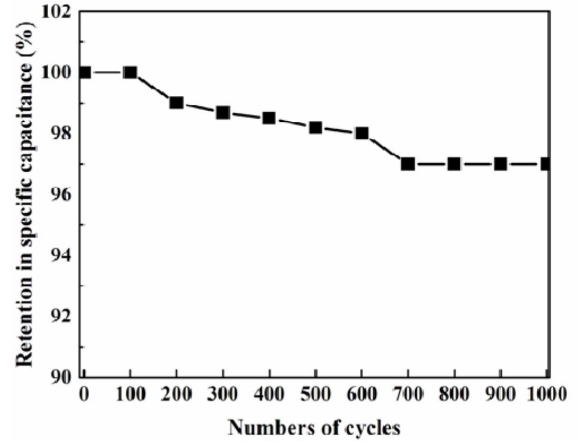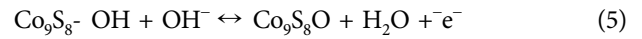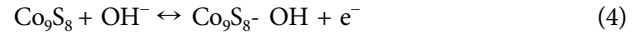

Fig. 7. Charge-discharge cyclic stability profile of CSRG

the following reversible reaction [17].

$$Co_9S_8 + OH^- \leftrightarrow Co_9S_8\text{-}OH + e^- \qquad (4)$$

$$Co_9S_8\text{-}OH + OH^- \leftrightarrow Co_9S_8O + H_2O + {}^-e^- \qquad (5)$$

The pseudocapacitance of Co_9S_8 combined with the EDLC of RGO in the CSRG composite, which shows high electrochemical properties. The energy and power density of both the compound were calculated by using the equation,

$$Energy\ density\ (E) = 1/8(CV^2) \qquad (6)$$

$$Power\ density = E/\Delta t \qquad (7)$$

The energy density of pure Co_9S_8 and CSRG were found to be 25.2 and 13.6 Wh kg^{-1} at a power density of 1000 W kg^{-1} respectively. The energy density found to be ~ 1.8 Wh kg^{-1} at a high power density of ~2500 W kg^{-1}.

In order to further characterise the electrochemical performances EIS was performed in the frequency range of 10^4-1 Hz with 10 mV sinusoidal DC bias. A semicircle was formed at the higher frequency region of CSRG, indicated very good capacitive behaviour. The solution resistant (SR) was calculated from the X- axis intercept of the Nyquist. The SR of pure Co_9S_8 and CSRG were found to be 1.3 and 6.6 Ω respectively. At the lower frequency region the imaginary part increased sharply with a lower Warburg resistance for CSRG than pure Co_9S_8. The improvement of SC value in the CSRG composite is attributed to the distinctive structure of the nano composites. The charge-discharge cyclic stability is an important parameter for the real application of the supercapacitor. The charge-discharge cycles are performed up to 1000 cycles at a current density of ~5 A g^{-1} (Fig. 7). It is noticed that the SC values decreased with no of cycles. The retention of SC is found to be ~98% after 500 cycles and finally it is found ~97% after 1000 charge-discharge cycles. The decrease of SC with no of cycles may be due to the partial ir-reversibility of the corresponding redox reactions. In order to obtain high working potential 4 symmetric devices were connected in a series and
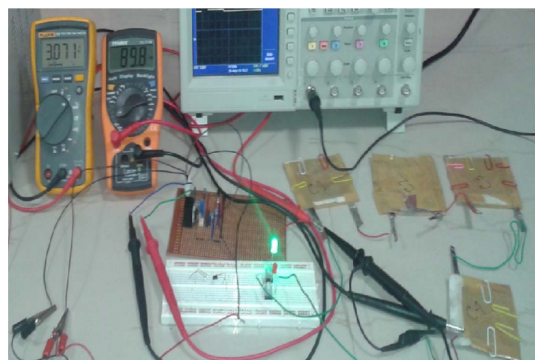
Fig. 8. Digital photograph of four symmetric devices in a series

the total system, which successfully powered a green LED, provided a working potential ~3.1 V (Fig. 8).

4. CONCLUSIONS

CSRG composite provides high supercapacitive properties. The FT-IR spectra reveals the reduction of GO and formation of Co_9S_8 by the two step hydrothermal method. The rod like Co_9S_8 decorated over RGO sheets are clearly visible from the FE-SEM and TEM images. The polycrystalline nature is observed by the SAED pattern image of CSRGO. The well exfoliated RGO sheets and the randomly oriented Co_9S_8 nano rods provide well electrode to electrolyte interaction. The RGO is used here as a binder and as well as conducting spacer to the Co_9S_8 nano rods. It is assumed that the redox nature of Co_9S_8 with EDLC nature of RGO synergistically provided the higher supercapacitive performances in CSRG composite. The high electrical conductivity ~98 S m^{-1} of CSRG confirms the reduction of GO by the hydrothermal reaction. The CSRG device exhibits a high specific capacitance ~728 F g^{-1} at a current density of 2 A g^{-1} with an energy density of ~25.2 Wh kg^{-1} at a power density of 1000 W kg^{-1}. The retention in Sc for CSRG is ~97% after 1000 charge-discharge cycles. Overall an easy way is reported to prepare a conductive electrode material to fabricate a high performance supercapacitor.

ACKNOWLEDGEMENT

REFERENCES

1. Chen, S.-M., Ramachandran, R., Mani, V., and Ramiah, S., "Recent Advancements in Electrode Materials for the High-performance Electrochemical Supercapacitors: A Review", *International Journal of Electrochemical Science*, Vol. 9, 2014, pp. 4072-4085.

2. Zhong, C., Deng, Y., Hu, W., Qiao, J., Zhang, L., and Zhang, J., "A Review of Electrolyte Materials and Compositions for Electrochemical Supercapacitors" *Chemical Society Reviews*, Vol. 44, No. 21, 2015, pp. 7484-7539.

3. Peng, X., Peng, L., Wu, C., and Xie, Y., "Two Dimensional Nanomaterials for Flexible Supercapacitors", *Chemical Society Reviews*, Vol. 43, No. 10, 2014, pp. 3303-3323.

4. Chen, T., and Dai, L., "Flexible Supercapacitors Based on Carbon Nanomaterials", *Journal of Materials Chemistry A*, Vol. 2, No. 28, 2014, pp. 10756-10775.

5. Tan, Y.B., and Lee, J.-M., "Graphene for Supercapacitor Applications", *Journal of Materials Chemistry A*, Vol. 1, No. 47, 2013, pp. 14814-14843.

6. Yu, Z., Tetard, L., Zhai, L., and Thomas, J., "Supercapacitor Electrode Materials: Nanostructures from 0 to 3 Dimensions", *Energy & Environmental Science*, Vol. 8, No. 3, 2015, pp. 702-730.

7. Conway, B.E., Electrochemical Supercapacitors, Plenum Publishing, New York, 1999.

8. Pu, J., Wang, Z., Wu, K., Yu, N., and Sheng, E., "Co_9S_8 Nanotube Arrays Supported on Nickel Foam for High-performance Supercapacitors," *Physical Chemistry Chemical Physics*, Vol. 16, No. 2, 2014, pp. 785-791.

9. Hu, C.C., Chang, K.H., Lin, M.C., and Wu, Y.T., "Design and Tailoring of the Nano Tubular Arrayed Architecture of Hydrous RuO_2 for Next Generation Supercapacitors" *Nano Letters*, Vol. 6, No. 12, 2006, pp. 2690-2695.

10. Zhang, D., and Zou, W., "Decorating Reduced Graphene Oxide with Co_3O_4 Hollow Spheres and Their Application in Supercapacitor Materials," *Current Applied Physics,* Vol. 13, No. 48, 2013, pp. 1796-1800.

11. Ramachandrana, R., Saranyaa, M., Santhosha, C., Velmurugana, V., Raghupathy, B.P.C., Jeong, S.K., and Gracea, A.N., "Co_9S_8 Nanoflakes on Graphene (Co_9S_8/G) Nanocomposites for High Performance Supercapacitors," *RSC Advance*, Vol. 4, No. 40, 2014, pp. 21151-21162.

12. Zhang, L., Wu, H.B., and Lou, X.W., "Unusual CoS_2 Ellipsoids with Anisotropic Tube-like Cavities and Their Application in Supercapacitors," *Chemical Communications*, Vol. 48, No. 55, 2012, pp. 6912-6914.

13. Jana, M., Khanra, P., Murmu, N.C., Samanta, P., Lee, J.H., and Kuila, T., "Covalent Surface Modification of Chemically Derived Graphene and Its Application as Supercapacitor Electrode Material," *Physical Chemistry Chemical Physics*, Vol. 16, No. 16, 2014, pp. 7618-7626.

14. Wang, Q., Jiao, L., Du, H., Yang, J., Huan, Q., Peng, W., Si, Y., Wang, Y., and Yuan, H., "Facile Synthesis and Superior Supercapacitor Performances of Three-dimensional Cobalt Sulfide

Hierarchitectures", *Cryst Eng Comm,* Vol. 13, No. 23, 2011, pp. 6960-6963.

15. Huang, S., Jin, Y., and Jia, M., "Preparation of Graphene/Co_3O_4 Composites by Hydrothermal Method and Their Electrochemical Properties", *Electrochimica Acta*, Vol. 95, 2013, pp. 139-145.

16. He, G., Wang, L., Chen, H., Sun, X., and Wang, X., "Preparation and Performance of $NiCo_2O_4$ Nano Wires-loaded Graphene as Supercapacitor Material", *Materials Letters,* Vol. 98, 2013, pp. 164-167.